CLASSIFICATION OF FLUCTUATING TURBULENT FLOWS

M. M. Grigor'ev, V. V. Kuz'min,
and A. V. Fafurin

UDC 532.526

The existence is shown of five different forms of the appearance of superposed fluctuations on flow characteristics on the basis of an analysis of the mechanism of turbulence propagation in fluctuating flows.

INTRODUCTION

A sufficiently large quantity of papers [1-30] is already devoted to the study of fluctuating turbulent flows (FTF); however, despite the efforts undertaken, the single-valued comprehension of many aspects of this interesting hydrodynamic phenomenon has still not been achieved. The first attempt at FTF classification is due to Carr [31], who proposed separating the FTF according to the nature and degree of appearance of dynamic effects into three qualitatively different categories on the basis of an analysis of the materials [8, 10, 11, 16, 17, 24, 32, 33]: flows in which the discharge fluctuations exert no influence, in practice, on the velocity distribution <u>; flows in which this influence is manifested locally in the near-wall layers; and flows in which it is propagated over the whole transverse section of the channel. Carr proposed as parameters characterizing the degree of appearance of the effect the relative amplitude β of the velocity fluctuations and the ratio f/f_e between the frequency of the superposed fluctuations f and the characteristic "explosion frequency" f_e. For the stationary case the "explosion frequency" is found experimentally in [34] in the form

$$f_e = \frac{\bar{u}_0}{5\bar{\delta}}, \tag{1}$$

where δ and $\bar{u}_0$ are mean values, in time, of the fluctuating turbulent boundary layer thickness and the velocity on its outer boundary.

It is proposed to classify the FTF according to the Strouhal number $St_\delta = \bar{f}\bar{\delta}/\bar{u}_0$ and β in [31]. However, both these approaches do not disclose the physical mechanism of the influence of the superposed fluctuations on the flow microstructure and do not afford a possibility of setting up a clear boundary between the second and third FTF categories.

A clearer FTF classification is proposed in [23] on the basis of the principle of turbulence propagation. The so-called "turbulent Stokes number" $(\omega/2\nu_T)^{1/2}D/2$ is introduced to estimate the velocity of turbulent kinetic energy (TKE) propagation and the extent of the TKE propagation zone y is formulated as a function of the turbulent viscosity ν_T and the time t:

$$y = \sqrt{\nu_T t}. \tag{2}$$

Assuming the turbulent viscosity in the outer boundary layer domain [35] constant and equal to

$$\nu_T = 0{,}007\, R\bar{u}_*, \tag{3}$$

the authors of [23] obtained a condition for turbulence propagation along the channel axis per period of discharge fluctuation

$$\frac{\omega D}{\bar{u}_*} \approx 0{,}88. \tag{4}$$

According to this classification, all the known FTF as a function of values of the complexes $\omega D/\bar{u}_*$ and $\bar{Re}_m$ and the nature of the appearance of nonstationary effects are separated into five groups, "quasistationary", "low-frequency", "medium-frequency", "high-

S. M. Kirov Kazan' Chemical-Technological Institute. Translated from Inzhenerno-Fizicheskii Zhurnal, Vol. 59, No. 5, pp. 725-735, November 1990. Original article submitted May 24, 1988.

0022-0841/90/5905-1359$12.50

frequency", and "rapidly oscillating" flows. Included in the first group are FTF characterized by no influence of nonstationarity on both the average and the fluctuation characteristics. Flows for which the influence of nonstationarity on just the distribution of $\langle u \rangle$ over the channel radius is characteristic are in the second group. The FTF characterized by noticeable interaction between the turbulent structure and the superposed oscillations, significant deformations of the turbulent velocity fluctuations profiles but quite a slight distinction between the distributions of the time-averaged velocities and the quasistationary analogs over the whole tube section fall into the third group. Flow for which a strong interaction between the turbulence and the stream oscillations is characteristic falls into the group of so-called "high-frequency" FTF. The influence of flow fluctuations on their turbulent structure is concentrated in a relatively narrow near-wall layer $y/R \leq 0.1$, while the turbulence outside this layer is "frozen" (oscillations occur according to the laws of a solid body). Inflection points can appear in profiles of the velocity $\bar{u}$ in flows of this group because of deformation of the kinetic structure. Among the "rapidly oscillating" are FTF in which turbulent structure interaction with the superposed oscillations in the near-wall layers appears most strongly while the transverse dimension of the domain of "frozen" turbulence exceeds by several times the dimensions of analogous FTF domains of the previous group.

The FTF classification made in [23] is an absolutely significant contribution to the comprehension of their nature. However, utilization of the complexes $\omega D/\bar{u}_*$ and $\overline{Re}_m$ as criteria for the referral of real FTF to some classification group is not completely legitimate since the approach does not here take account of one quite important circumstance, the influence of the amplitude of the superposed fluctuations on the average and fluctuating (turbulent) flow characteristics. For this reason the predictions of the authors of [23] relative to the boundaries of the domains of existence of the FTF groups listed are probably not in agreement with existing experimental data.

1. MECHANISM OF TURBULENCE PROPAGATION IN FTF

It is known that the main fraction of the TKE in stationary turbulent boundary layers (TBL) is generated in the near-wall domains ($y^+ = y\bar{u}_*/\nu = 10\text{-}12$), where the generation is related to renewal of the viscous sublayer [34-36], is explosive in nature, and is repeated at a definite frequency on the average. According to the data in [34], the mean frequency of viscous sublayer renewal and of turbulence "explosions" accompanied by ejections of turbulent formations from the domain of TKE generation is determined by the dependence (1). The turbulent formations that are carriers of a definite quantity of TKE are propagated over the whole stream thickness at certain finite velocities because of diffusion and convection. To determine their propagation rates v_p for stationary flow regimes, information would be required about the evolutions of instantaneous states of the whole flow field; however, it is a quite complex matter and not realizable in practice to obtain such information at this time.

In the case of nonstationary periodic (in particular, fluctuating) turbulent flows, the question of determining v_p is simplified noticeably and can be solved by using modern diagnostic apparatus with an automated statistical signal processing method.

It is necessary to have the velocity field $\langle u \rangle$ and the turbulent tangential stresses $\langle u'v' \rangle$ averaged over the ensemble of realization in different phases of discharge fluctuations of the working medium as the initial data to determine the quantity of TKE being generated

$$P = \langle u'v' \rangle \frac{d \langle u \rangle}{dr}$$

in a fluctuating turbulent flow.

The changes in the quantity $RP/\bar{u}_*^3$ over the period and over the thickness of the fluctuating boundary layer can be assessed from the constant level lines of the TKE generation density represented in Fig. 1. These data are obtained on an installation [7] by using a two-channel thermoanemometer of constant temperature and an automated measuring-calculating complex [37]. The measurements were executed in a D = 50 mm diameter cylindrical channel in a section with the coordinate x = 45D corresponding to developed fluctuating turbulent flow. The stream fluctuations were realized in a sinusoid with frequency $f = 1/T = 3$ Hz and $\beta_{um} = 50\%$ relative amplitude. The mean-discharge Reynolds number determined as $\overline{Re}_m = \bar{u}_m D/\nu$ was 25,500.

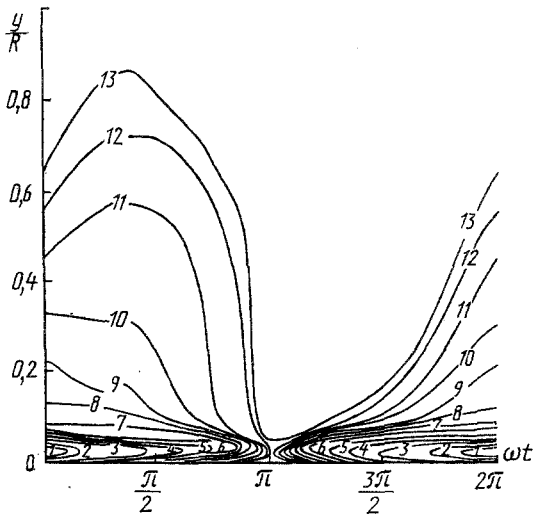

Fig. 1. Change in density of TKE generation over a period of discharge fluctuation and over the tube radius. 1) $RP/\overline{u}_*^3$ = 200; 2) 175; 3) 150; 4) 125; 5) 100; 6) 75; 7) 50; 8) 40; 9) 30; 10) 20; 11) 10; 12) 5; 13) 2.5.

The deduction can be made from Fig. 1 that the maximal density of turbulent energy and turbulence "explosion" generation accompanied by ejections of the most energy-containing formations in the flow during fluctuating medium motion would occur in the maximum discharge phase in the near-wall flow layers where the maximal values of the turbulent tangential stresses $\langle u'v' \rangle$ would be combined with the maximal velocity gradient $\partial\langle u \rangle/\partial r$. The level of TKE generation in this phase (at the identical coordinate y) would exceed by several tens of times the value P in the phase of the discharge velocity minimum.

The TKE being generated in the near-wall domain of a fluctuating flow (in the domain of the viscous sublayer outer boundary) in the above-mentioned phase of $\langle u_m \rangle$ change is propagated over the flow core and the viscous sublayer at a certain finite velocity. This latter circumstance is the reason that the fluctuations in the turbulent kinetic energy values lag in phase behind the fluctuations of the mean-discharge velocity $\langle u_m \rangle$, where this lag increases monotonically in the direction of the channel axis [2, 10, 12, 23, 25-26, 28-30].

If the turbulence propagation velocity is understood to be the displacement velocity of the most energy-containing formations from their generation zone, then its magnitude can be determined by using the data in [18]. The time Δt of turbulence propagation over the whose turbulent boundary layer section was determined in this paper on the basis of measuring the auto-correlation functions. According to the data in [18], the time of turbulence propagation Δt_0 from the zone of TKE generation to the tube axis would agree with the mean value of the period T_e of the explosion of turbulence. The experimental results presented in [18] are generalized satisfactorily by a dependence of the form

$$\lg \overline{\Delta t^+} = \lg \bar{y}^+ + \lg 2, \tag{5}$$

where

$$\overline{\Delta t^+} = \frac{\Delta t \bar{u}_*^2}{\nu}. \tag{6}$$

Substituting (6) into (5), we obtain the expression

$$\Delta t = \frac{2y}{\bar{u}_*}, \tag{7}$$

which is easily converted into the form

$$\frac{\Delta t \bar{u}_*}{D} = \frac{y}{R}. \tag{8}$$

The velocity of turbulence propagation is found from (7) and is written as

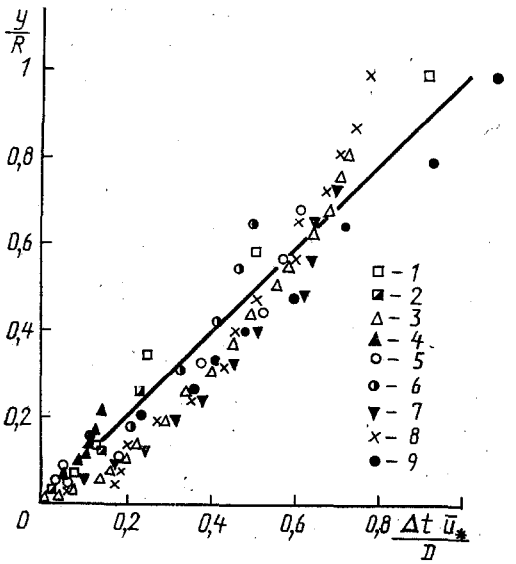

Fig. 2. Lag in the time of turbulent energy propagation in fluctuating flows: 1) data in [2] for $\overline{Re}_m$ = 32,000, βu_m = 50%, f = 1 Hz; 2) [2] for $\overline{Re}_m$ = 32,000, βu_m = 50%, f = 10 Hz; 3) [30] for $\overline{Re}_m$ = 50,000, f = 0.5 Hz; 4) [30], $\overline{Re}_m$ = 50,000, f = 3.6 Hz; 5) [28] for $\overline{Re}_m$ = 3900, f = 0.625 Hz; 6) [28] for $\overline{Re}_m$ = 5800, f = 0.625 Hz; 7) data of authors for $\overline{Re}_m$ = 25,000, f = 3 Hz, βu_m = 50%; 8) data of authors for $\overline{Re}_m$ = 25,500, f = 3 Hz, βu_m = 13.5%.

$$v_p = \frac{\bar{u}_*}{2}, \tag{9}$$

where $\bar{u}_*$ is the average value of the dynamic velocity over time. It follows from (9) that the velocity v_p is determined uniquely by the value of $\bar{u}_*$ and depends on neither the time nor the space coordinates.

This deduction is verified by comparing the dependence (8) shown by a straight line in Fig. 2 with the results of processing experimental material of the authors of this paper and data obtained by other researchers. The radial distributions of the phase angles of fluctuations of the TKE magnitudes <k> and the intensities of the longitudinal component intensities of the turbulent velocity fluctuations $\langle u'^2 \rangle$ obtained for different values of βu_m, $\overline{Re}_m$ presented in [2, 28, 30] were initial information to determine the values $\Delta t \bar{u}_*/D$ superposed in Fig. 2. The data 9 are obtained as a result of processing experimental results [7] on propagation of peak values of the excess coefficients. The spread of points from the dependence (8) in Fig. 2 does not exceed the error in determining the quantities used for their construction. It hence follows that the normalized velocity of turbulence propagation $v_p/\bar{u}_*$ in FTF is neither dependent on the frequency f nor the amplitude β_{um}, nor the Reynolds number $\overline{Re}_m$. Correspondingly, the velocity v_p depends only on the dynamic velocity $\bar{u}_*$.

The dependence (8) was later used to forecast possible modifications of turbulence propagation in fluctuating flows (Fig. 3). To do this it was first reduced to the form

$$\frac{y}{R} = \frac{\bar{u}_* T}{D} \frac{\Delta t}{T}. \tag{10}$$

The condition at which TKE batches generated in the near-wall domain reach the tube axis can be represented by the equality

$$\frac{\Delta t_0}{T} = \frac{D}{\bar{u}_* T} = \frac{fD}{\bar{u}_*}. \tag{11}$$

Line 1 in Fig. 3 corresponds to that fluctuating flow mode for which the TKE from the generation zone succeeds in being propagated over the whole flow thickness (to the tube axis) in the time $\Delta t_0 \ll T$. Here $fD/\bar{u}_* \to 0$, the phase shifts between the fluctuations of the velocity <u> (line a) and the quantities <k> (line b) are missing in practice and the flow characteristics correspond to quasistationary analogs.

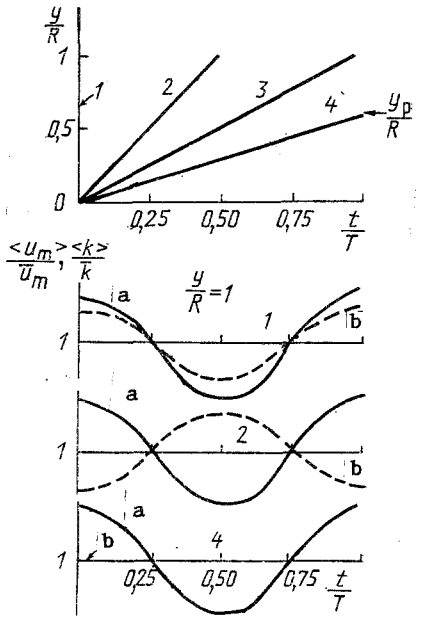

Fig. 3. Modifications of the turbulence propagation in fluctuating flows: a) $\langle u_m \rangle / \bar{u}_m$; b) $\langle k \rangle / k$.

As the value of the combination $fD/\bar{u}_*$ increases, the lag in turbulence propagation over the flow thickness becomes more and more noticeable (line 2 in Fig. 3). The flow characteristics (especially the fluctuating ones) start to deviate from the quasistationary values while the condition $\Delta t_0 < T$ is still conserved.

For $fD/\bar{u}_* = 1$ (line 3) the time of turbulence propagation in the whole flow thickness agrees with the period of working medium discharge fluctuation. Starting with this time, a "frozen" turbulence zone (line 4) appears in the FTF, which is characterized by invariance of the TKE in time. For such a flow mode, turbulence does not succeed in being propagated from the maximal generation zone in the whole flow thickness during the time T and, starting with a certain coordinate, its superposition on the turbulence generated in the previous period of velocity fluctuation occurs.

The distance y_p between the tube wall and the "frozen" turbulence zone can be calculated from the relationship (10) for $\Delta t = T$:

$$\frac{y_p}{R} = \frac{\bar{u}_* T}{D} = \frac{1}{fD/\bar{u}_*}, \qquad (12)$$

where $fD/\bar{u}_* \geq 1$.

The dependence (12) is shown by a line in Fig. 4. Data over the "frozen" turbulence layer thicknesses obtained by processing the experimental results in [2, 12, 16, 18, 25, 30] and the authors' data (see Tables 1 and 2 for the notation of the points) are represented here by points. Data referring to the FTF on a flat plate are also represented in Fig. 4. Twice the average thickness of the fluctuating turbulent boundary layer $2\bar{\delta}$ is used as the characteristic linear dimension instead of D during processing of the data referring to flows on flat plates.

The domain a in Fig. 4 corresponds to cases when $\Delta t_0 \leq T$ while the domain b is when $\Delta t_0 > T$. Two subdomains IV and V are provisionally separated out in domain b. Subdomain IV is bounded by the dimensionless frequencies $1 \leq fD/\bar{u}_* < 10$ while the "frozen" turbulence zone is extended in the space from $1 \geq y_p/R > 0.1$. For the subdomain V ($10 \leq fD/\bar{u}_* < 100$) the "frozen" turbulence is localized in the zone from $0.1 \geq y_p/R > 0.01$.

Comparing the dependence (4) presented in [23] and the dependence $fD/\bar{u}_* = 1$ obtained by the authors, that characterize the condition of turbulence propagation along the tube axis during one velocity fluctuation period $\langle u_m \rangle$, displays their substantial divergence. Earlier "frozen" turbulence is predicted by the dependence (4), which is not confirmed by the data presented in Fig. 4.

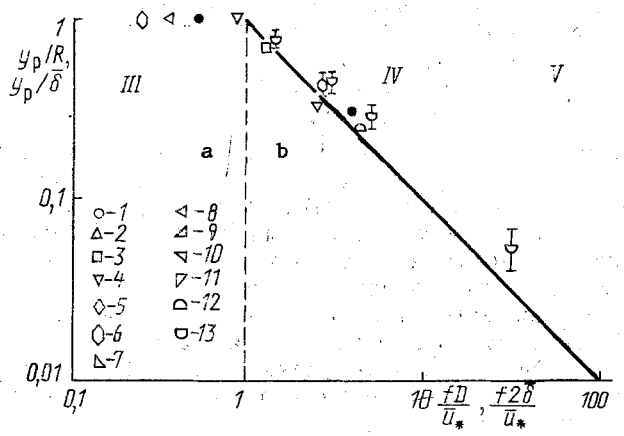

Fig. 4. Influence of the dimensionless frequency on the thickness of the turbulence propagation layer: open symbols without bars – regime 1; dark symbols without bars – regime 2; open symbols with upper bar – regime 3; dark symbols with horizontal bar regime 4; light symbols with bar below – regime 5.

TABLE 1. Information about Experimental Investigations of Fluctuating Turbulent Flows in a Tube

Source	$\overline{Re}_m$	f, Hz	$fD/\bar{u}_*$	β_{u_m}	Mode	Notation in Figs. 4 and 5
[30]	50000	0,5	0,49	0,64	3	1
		3,6	3,53	0,15	4	
[24]	2100	1,75	2,08	0,35	4	2
[12]	41800	1	0,804	0,073	2	3
	20100	1	1,27	0,197	4	
	28400	1	1,17	0,146	3	
	28800	0,5	0,586	0,088	2	
[18]	10000	0,62	2,45	0,42	4	4
		0,197	0,78	0,50	3	
[17]	10000	0,126	0,075	0,53	2	4
		0,757	0,45	0,75	3	
[28]	4000	0,208	0,05	0,07	1	5
		0,416	0,10	0,24	2	
		0,77	0,185	0,20	2	
		1,282	0,309	0,12	2	
	3900	0,625	0,154	0,10	2	
	5800	0,625	0,109	0,10	1	
	7500	0,625	0,087	0,10	1	
[1, 2]	32000	1	0,230	0,50	3	6
		10	2,39	0,50	4	
		10	2,43	0,20	4	
	64000	10	1,28	0,50	3	7
[15]	36000	2,08	0,179	0,522	2	
				0,802	3	
				0,257	2	
	35100	1,02	0,09	0,248	2	
	58700	2,08	0,117	0,533	2	
	84500	2,08	0,085	0,266	2	
	70300	2,08	0,099	0,334	2	
	36500	0,299	0,025	0,262	1	
Authors' data	25500	3	0,338	0,50	3	8
			0,34	0,135	2	

2. CLASSIFICATION OF FLUCTUATING TURBULENT FLOWS

It was mentioned above that effects associated with the influence of the relative amplitude of the discharge fluctuation were not taken into account in the classification of turbulent flow according to the parameters $\omega D/\bar{u}_*$ and $\overline{Re}_m$ presented in [23]. According to this classification, in FTF characterized by identical values of combinations $\omega D/\bar{u}_*$ and $\overline{Re}_m$, independently of β_{um} nonstationary effects should appear identical. However, practice has shown that this is not so. In particular, the authors of this paper saw this in an experimental investigation of developed turbulent air flows in a cylindrical tube, fluctuating at a f = 3 Hz frequency for Re_m = 25,500 for two different values of the discharge fluctuation amplitude β_{um} = 13.5 and 50%. According to the classification in [23], both these regimes

TABLE 2. Information about Experimental Investigations of Fluctuating Turbulent Boundary Layers on a Flat Plate or in a Plane Channel

Source	$\bar{\delta}$, m	f, Hz	$\frac{2f\bar{\delta}}{u_*}$	$\beta_{\langle u_0 \rangle}$	Mode	Notation in Figs. 4 and 5
[5]	0,05	0,25	1	0,05	3	9
		0,5	2	0,05	4	
		2	8	0,05	4	
[13]	0,05	0,314	0,33	1,0	3	10
[29]	0,0623	22	7,83	0,055	5	11
		24	8,54	0,055	5	
		26	9,25	0,055	5	
		29	10,3	0,055	5	
[25]	0,4	2	4,2	0,40	4	12
[16]	0,076	0,33	0,261	0,292	2	13
				0,202	2	
				0,147	2	
		0,66	0,448	0,34	3	
				0,149	2	
				0,112	2	
		1	0,678	0,352	3	
				0,195	3	
				0,107	3	
		1,33	0,902	0,344	3	
				0,215	3	
				0,13	3	
		2	1,36	0,286	4	
				0,176	4	
				0,081	3	
		4	2,71	0,264	4	
				0,136	4	
				0,062	3	
		7,65	5,19	0,297	4	
				0,127	4	
				0,073	4	
		48	32,6	0,34	5	

should be in the "medium frequency" group. However, if the superposed fluctuations on the profile of the velocity $\langle u \rangle$ were missing in practice in a flow with $\beta_{um} = 13.5\%$ and deformation of just the profiles of the turbulent fluctuation intensities $\langle u'^2 \rangle$ averaged with respect to the phase were observed, then for $\beta_{um} = 50\%$ substantial influence of nonstationary effects would be observed on the distributions of the quantities $\langle u'^2 \rangle$ and $\langle u \rangle$. Observations [15, 28] indicated that the fluctuation characteristics $\langle u'^2 \rangle$, $\langle v'^2 \rangle$, $\langle u'v' \rangle$ vary primarily under the influence of the superposed fluctuations and then as the dimensionless frequency $fD/\bar{u}_*$ or the amplitude β_{um} grows, noticeable deformations of the profiles of the velocities $\langle u \rangle$ and $\bar{u}_m$ appear.

The main characteristics of flows investigated in [2, 5, 12, 13, 15-18, 24, 25, 28-30] are represented in Tables 1 and 2. Analysis of the cited material permitted the authors of this paper to extract five different forms of the appearance of nonstationary effects in fluctuating flows, similarly to [23], and to classify the flows according to this criterion by division into separate groups.

As in [23], FTF in which the connections between the characteristics are subject to "quasistationary" regularities are included in the first group. The influence of the prehistory does not appear in flows of this kind while changes in the quantities $\langle u \rangle$, $\langle u'^2 \rangle$, and $\langle u_m \rangle$ occur practically cophasally.

The FTF in which nonstationary effects influence the TKE distribution over the boundary layer without noticeably deforming the field of the velocities $\langle u_m \rangle$ averaged over the ensemble are included in the second group of the proposed classification.

The principal feature of the FTF included in the third group is that the influence of nonstationary effects therein appears over the whole boundary layer thickness and is extended to both the TKE distribution and to the profile of $\langle u \rangle$. Profiles of the velocity $\bar{u}$ in the FTF of this group are deformed principally near the streamlined surface. As the dimensionless frequency $fD/\bar{u}_*$ or the relative amplitude β_{um} of the flow fluctuations increases, the influence of the nonstationary effects grows.

The fourth FTF group is characterized by the still more substantial influence of the flow fluctuations on the flow configuration and the localization of this influence in the

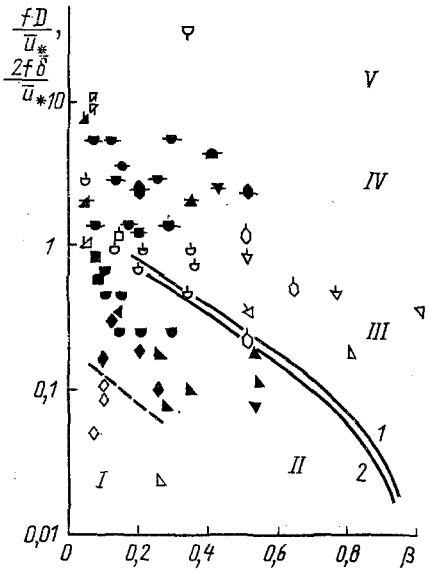

Fig. 5. Classification of nonstationary turbulent flows (notation the same as in Fig. 4).

layer $0 < y_p/R \leq \bar{u}_*/(FD)$. Inflection points appear in the $\bar{u}$ profiles near the wall, and "frozen" turbulence in the domain $y_p > \bar{u}_*/(2f)$.

The distinctive feature of the FTF of the fifth group of the proposed classification is that the influence of nonstationarity therein is concentrated in a quite thin near-wall layer $0 < y/R < 0.1$. This type of flow has as yet been investigated least.

In conformity with the FTF classification taken, the data from Tables 1 and 2 were superposed in Fig. 5. The symbols corresponding to the different FTF groups occupy definite domains in the plane $fD/\bar{u}_*$, β. The boundaries between domains III, IV and IV, V are found from the condition for the existence of a "frozen" turbulence layer and are represented, respectively, in the form $fD/\bar{u}_* = 1$ and $fD/\bar{u}_* = 10$.

Determination of the boundary between domains II and III was the most complex problem. The fact set up experimentally [7] that the characteristic feature of fluctuating flows of the third group and the principal reason for the anomalies observed here in the distributions of the velocity $\langle u \rangle$ are the quite definite delay in the reaction of the turbulent flow configuration to a change in the velocity $\langle u_m \rangle$, the so-called hysteresis of turbulence, was used in solving this problem. This phenomenon occurs because of the significant magnification of nonstationary convection mechanism and the introduction of turbulent kinetic energy by this mechanism from the phases of flow retardation, where it is generated intensively and does not succeed completely in dissipation, to the phase, of the minimum and the increase of the discharge.

Analysis of the TKE balance shows that the state of local equilibrium of turbulence can be disturbed when the nonstationary convection of turbulent kinetic energy becomes commensurate with the other terms of the balance equation, in particular, the dissipative term. This condition can be represented as follows

$$\frac{\partial \langle k_q \rangle}{\partial t} \cong \langle \varepsilon_q \rangle, \tag{13}$$

where $\langle k_q \rangle$ is the quasistationary TKE value and $\langle \varepsilon_q \rangle$ is the TKE dissipation.

Let us reduce the left and right sides of (13) to dimensionless form by multiplying them by $R/\langle u_* \rangle^3$;

$$\Phi = \frac{R}{\langle u_* \rangle^3} \frac{\partial \langle k_q \rangle}{\partial t} \simeq \frac{R}{\langle u_* \rangle^3} \langle \varepsilon_q \rangle. \tag{14}$$

According to the data in [35, 38],

$$\frac{R}{\langle u_* \rangle^3} \langle \varepsilon_q \rangle \simeq 2 \tag{15}$$

on the tube axis for a stationary turbulent flow regime while according to the data in [35], for r = 0

$$\langle k_q \rangle^{1/2} / \langle u_m \rangle \cong 0{,}05. \tag{16}$$

Substitution of (16) into (14) and replacement of $\langle u_* \rangle$ by the hydraulic drag coefficient by using the relationship

$$\langle u_* \rangle = \langle u_m \rangle \sqrt{\langle \lambda \rangle / 8} \tag{17}$$

for a turbulent flow fluctuating according to the law $\langle u_m(\omega t) \rangle = \bar{u}_m(1 + \beta_{um} \cos \omega t)$ yields

$$\Phi = -0{,}005 \left(\frac{\langle \lambda \rangle}{8} \right)^{-3/2} R \bar{u}_m \beta \omega \sin \omega t / \langle u_m \rangle^2. \tag{18}$$

Let us determine the angle ωt, for which the function (18) takes on the maximal value

$$(\omega t)_{\max} = \arccos \left(\frac{1 - \sqrt{1 + 8\beta^2}}{2\beta} \right). \tag{19}$$

Substituting (19) into (18) and taking (15) and (14) into account, we obtain

$$\frac{fD}{\bar{u}_*} = \frac{(1 + \beta \cos (\omega t)_{\max})^2 (\langle \lambda \rangle / 8)^{3/2}}{\sin (\omega t)_{\max} \, 0{,}005 \pi \beta \sqrt{\bar{\lambda}/8}}. \tag{20}$$

The quantity $\langle \lambda \rangle$ in (20) is calculated from (17) for the phase $(\omega t)_{\max}$. The right side of (20) depends only on $\overline{Re}_m$ and β.

A computation using (20) for $\overline{Re}_m$ = 50,000 and 25,000 is represented by lines 1 and 2, respectively, in Fig. 5. The insignificant stratification of the lines 1 and 2 indicates that the value of the complex $fD/\bar{u}_*$ depends weakly on $\overline{Re}_m$. The behavior of curves 1 and 2 in Fig. 5 indicates a tendency to broadening of the zone of regime 3 existence as the flow fluctuation amplitudes increase.

NOTATION

x, r are cylindrical coordinates; y is the coordinate measured from the wall; u, v are velocity components along the x, r axes; t is the time; R is the tube radius; D is the diameter; δ is the boundary layer thickness; f is the frequency; ω is the cyclic frequency; T is the period; u_* is the dynamic velocity; u_0 is the velocity on the tube axis or in the external flow; ν is the kinematic viscosity; ν_T is the turbulent viscosity; R_e is the Reynolds number; u_m is the mean mass flow rate; v_p is the velocity of turbulence propagation; $\langle u'^2 \rangle$, $\langle v'^2 \rangle$, $\langle w'^2 \rangle$ are values of the turbulent velocity component fluctuations averaged over the ensemble; $\langle k \rangle = (\langle u'^2 \rangle + \langle v'^2 \rangle + \langle \omega'^2 \rangle)/2$ is the turbulent kinetic energy; $\langle u'v' \rangle$ is the turbulent tangential stress; β is the fluctuation amplitude; y_p is the thickness of the turbulence propagation layer; ε is the dissipation rate; λ is the hydraulic drag coefficient; P is the turbulent energy generation. Subscripts: 0 is for values on the tube axis; q is for the quasistationary value; m is for the mean discharge velocity; * is for the dynamic velocity; ( )' is for turbulent fluctuations. Symbols: < > is for averaging over the ensemble, upper bar is for averaging with respect to time.

LITERATURE CITED

1. V. I. Burkreev and V. M. Shakhin, Aeromekhanika [in Russian], Moscow (1976), pp. 180-187.
2. V. I. Bukreev and V. M. Shakhin, Statistically Nonstationary Turbulent Flow in a Tube [in Russian], Dep. No. 866-81, VINITI, Moscow (1981).
3. J. Cousteix, A. Desopper, and R. Houdeville, Turbulent Shear Flows [Russian translation] Part I, Moscow (1982), pp. 159-177.
4. S. B. Markov, Izv. Akad. Nauk SSSR, Mekhan. Zhidk. Gaza, No. 2, 65-74 (1973).
5. P. G. Parikh, W. C. Reynolds, and R. Jayaraman, Aerospace Engineering [Russian translation], 1, No. 1, 73-80 (1983).
6. B. V. Perepelitsa and Yu. M. Pshenichnikov, Structure of Hydrodynamic Flows [in Russian], Novosibirsk (1986), pp. 14-24.

7. M. M. Grigor'ev and A. V. Kostromin, Modern Thermophysics Problems [in Russian], Novosibirsk (1987), pp. 280-291.
8. M. Acharya and W. C. Reynolds, Tech. Rep. TF-8, Stanford Univ. Thermosci. Div. (1975).
9. G. Binder and J. L. Kueny, Turbulent Shear Flow. 3. Selected Papers from the Third Intern. Symp. on Turb. Shear Flows, 6-17 (1981).
10. J. Cousteix, R. Houdeville, and J. Javelle, IUTAM Symp. Unsteady Turb. Shear Flows, Toulouse, France, pp. 120-144 (1981).
11. J. Cousteix, A. Desopper, and R. Houdeville, Rech. Aerosp., No. 3, 167-177 (1977).
12. E. Hartner, Doctoral Dissertation, Feb. 21, 1984. TU, Munchen (1984).
13. M. Hino, M. Kashiwayanagi, A. Nakayama, and T. Hara, J. Fluid Mech., 131, 363-400 (1983).
14. R. Houdeville and J. Cousteix, Rech. Aerosp., No. 1, 33-48 (1979).
15. M. Iguchi, M. Ohmi, and S. Tanaka, Bull. ISME, 28, No. 246, 2915-2922 (1985).
16. S. K. F. Karlsson, J. Fluid. Mech., 5, 622-636 (1959).
17. T. Mizushina, T. Maruyama, and Y. Shiozaki, J. Chem. Eng. Japan, 6, No. 6, 487-494 (1975).
18. T. Mizushina, T. Maruyama, and H. Hirasawa, J. Chem. Eng. Japan, 8, No. 3, 210-216 (1975).
19. M. Ohmi and M. Iguchi, Bull. ISME, 23, No. 186, 2013-2020 (1983).
20. M. Ohmi and M. Iguchi, Bull. ISME, 23, No. 186, 2021-2028 (1983).
21. M. Ohmi, S. Kyomen, M. Iguchi, and T. Usui, Tech. Rep., 33, No. 1729, 359-365, Osaka Univ. (1983).
22. M. H. Patel, Proc. Roy. Soc. London, A, No. 353, 121-144 (1977).
23. B. R. Ramaprian and S. W. Tu, J. Fluid Mech., 137, 59-81 (1983).
24. B. R. Ramaprian and S. W. Tu, J. Fluid Mech., 100, 513-544 (1980).
25. B. R. Ramaprian, S. W. Tu, and A. N. Menendez, Turb. Shear Flows, 4. Sel. Papers, Fourth Intern. Symp. Turb. Shear Flows, Karsruhe Univ., pp. 301-310 (1983).
26. B. R. Ramaprian and S. W. Tu, IUTAM Symp. Unsteady Turb. Shear Flows, Toulouse, France, pp. 47-57 (1981).
27. L. Shemer and E. Kit, Phys. Fluids, 27, No. 1, 72-76 (1984).
28. L. Shemer, I. Wygnanski, and E. Kit, J. Fluid Mech., 153, 313-337 (1983).
29. J. Tartarin, Revue Phys. Appl., 18, 495-505 (1983).
30. S. W. Tu and B. R. Ramaprian, J. Fluid Mech., 137, 31-58 (1983).
31. L. W. Carr, IUTAM Symp. Unsteady Turb. Shear Flows, May 5-8, Toulouse, France, 5-34 (1981).
32. P. G. Parikh, W. C. Reynolds, R. Jayaraman, and W. Carr, IUTAM Symp. Unsteady Turb. Shear Flows, Toulouse, France, pp. 35-46 (1981).
33. R. I. Simpson, B. G. Shivaprasad, and Y. T. Chew, IUTAM Symp. Unsteady Turb. Shear Flow, Toulouse, France, pp. 109-119 (1981).
34. K. N. Rao, R. Narasimha, M. A. Badri Narayanan, J. Fluid Mech., 48, 339-352 (1971).
35. J. O. Hintse, Turbulence, Its Mechanism and Theory [Russian translation], Moscow (1963).
36. E. U. Repik and Yu. P. Sosedko, Aeromekhanika [in Russian], 170-180, Moscow (1976).
37. A. S. Livshits, V. M. Loskutov, V. V. Kuz'min, et al., Two-Level Measuring-Calculating Complex for the Experimental Investigation of Nonstationary Turbulent Flows [in Russian], Kazan', 1987. Dep. No. 5286-B87 in VINITI, July 22, 1987 (1987).
38. J. Laufer, NACA Rep. No. 1174, 489-513 (1954).